

Transcriptional regulation of phagocytosis-induced membrane biogenesis by sterol regulatory element binding proteins

Adam B. Castoreno*[†], Yan Wang*[†], Walter Stockinger*, Larissa A. Jarzylo*, Hong Du[‡], Joanne C. Pagnon*, Eugenie C. Shieh*, and Axel Nohturfft*[§]

*Department of Molecular and Cellular Biology, The Biological Laboratories, Harvard University, 16 Divinity Avenue, Cambridge, MA 02138; [†]The Children's Hospital Research Foundation of Cincinnati Children's Hospital Medical Center, 3333 Burnet Avenue, Cincinnati, OH 45229

Communicated by Raymond L. Erikson, Harvard University, Cambridge, MA, August 4, 2005 (received for review July 7, 2005)

In the process of membrane biogenesis several dozen proteins must operate in precise concert to generate ≈ 100 lipids at appropriate concentrations. To study the regulation of bilayer assembly in a cell cycle-independent manner, we have exploited the fact that phagocytes replenish membranes expended during particle engulfment in a rapid phase of lipid synthesis. In response to phagocytosis of latex beads, human embryonic kidney 293 cells synthesized cholesterol and phospholipids at amounts equivalent to the surface area of the internalized particles. Lipid synthesis was accompanied by increased transcription of several lipogenic proteins, including the low-density lipoprotein receptor, enzymes required for cholesterol synthesis (3-hydroxy-3-methylglutaryl CoA synthase, 3-hydroxy-3-methylglutaryl CoA reductase), and fatty acid synthase. Phagocytosis triggered the proteolytic activation of two lipogenic transcription factors, sterol regulatory element binding protein-1a (SREBP-1a) and SREBP-2. Proteolysis of SREBPs coincided with the appearance of their transcriptionally active N termini in the nucleus and 3-fold activation of an SREBP-specific reporter gene. In previous studies with cultured cells, proteolytic activation of SREBP-1a and SREBP-2 has been observed in response to selective starvation of cells for cholesterol and unsaturated fatty acids. However, under the current conditions, SREBP-1a and SREBP-2 are induced without lipid deprivation. SREBP activation is inhibited by high levels of the SREBP-interacting proteins Insig1 or the cytosolic domain of SREBP cleavage-activating protein. Upon overexpression of these proteins, phagocytosis-induced transcription and lipid synthesis were blocked. These results identify SREBPs as essential regulators of membrane biogenesis and provide a useful system for further studies on membrane homeostasis.

gene regulation | lipid synthesis | organelle biogenesis

Membrane synthesis involves the concerted assembly of lipids in organelle and cell type-specific proportions (1). Although the biochemical steps of membrane lipid synthesis are well understood, little is known about the mechanisms by which different pathways are coordinated to produce bilayers of appropriate composition.

To facilitate investigations into the coordination of membrane biogenesis as an isolated process, it would be desirable to choose an experimental system in which bilayer synthesis occurs inducibly, extensively, and uncoupled from cell growth, differentiation, and hormonal control. One cell type that meets these criteria are phagocytes. In the course of phagocytosis, a patch of membrane is wrapped around an external particle and internalized to form a phagosome (2). To maintain constant surface area, plasma membrane lipids that are consumed during particle uptake are simultaneously replenished from intracellular organelles (3). In primary mouse macrophages, phagocytosis of latex beads proceeds until cellular membrane stores are exhausted (4). After a lag period of ≈ 3 h, macrophages begin to synthesize new membranes and recover the ability to engulf more

particles (4). Phagocytosis-induced lipid synthesis in macrophages requires ongoing transcription, suggesting that phagocytosis might offer a useful opportunity to study the regulatory mechanisms that induce and coordinate the synthesis of membranes.

Here we show that phagocytosis of latex beads by human embryonic kidney 293 cells is followed by a rapid phase of membrane synthesis similar to what has been reported for mouse macrophages. Lipid synthesis is accompanied by increased transcription of the genes for the LDL receptor and for enzymes that catalyze key steps in cholesterol and fatty acid synthesis. Phagocytosis-induced transcription and lipid synthesis are shown to require the activity of sterol regulatory element binding protein (SREBP) transcription factors. These results identify SREBPs as central regulators of membrane biogenesis.

Materials and Methods

Reagents. We obtained latrunculin A and compactin from Sigma; hydroxypropyl β -cyclodextrin from Cyclodextrin Technologies Development (High Springs, FL); 25-hydroxycholesterol (25HC) from Steraloids; [³H]cholesteryl oleate from PerkinElmer; yttrium silicate beads from GE Healthcare; FBS from Invitrogen, and other cell culture reagents from Mediatech. Monoclonal antibodies IgG-2A4 and IgG-1D2 against the N termini of human SREBP-1a (5) and SREBP-2 (6), respectively, were kindly provided by Y. K. Ho (University of Texas Southwestern Medical Center, Dallas). Lipoprotein-deficient FBS (LPDS) was prepared as described (7).

Buffers. PBS refers to phosphate-buffered saline at pH 7.4. TBS refers to 20 mM Tris-HCl (pH 7.5) plus 150 mM NaCl. Buffer A contains 20 mM Tris-HCl (pH 7.8), 10% (vol/vol) glycerol, 3 mM DTT, and 0.5% (vol/vol) Triton X-100 plus protease inhibitors (520 μ M AEBSF/0.4 μ M aprotinin/10 μ M leupeptin/20 μ M bestatin/7.5 μ M pepstatin A/7 μ M E-64) (Sigma). Buffer B contains 10 mM Tris-HCl (pH 7.6), 10 mM NaCl, and 1% (wt/vol) SDS plus protease inhibitors.

Isolation of Immortalized Mouse Macrophages (HD1A Cells). Peritoneal macrophages were collected from male mice that had been generated through a cross with ImmortoMice (Charles River Laboratories) expressing a temperature-sensitive version of simian virus 40 large T antigen from an IFN- γ inducible promoter (8). Cell suspensions were obtained by peritoneal lavage with 8 ml of PBS, washed, and cultured at 33°C in RPMI medium 1640

Abbreviations: SREBP, sterol regulatory element binding protein; 25HC, 25-hydroxycholesterol; LPDS, lipoprotein-deficient FBS; HMG, 3-hydroxy-3-methylglutaryl; LDL, low-density lipoprotein; FAS, fatty acid synthase; ER, endoplasmic reticulum.

[†]A.B.C. and Y.W. contributed equally to this work.

[§]To whom correspondence should be addressed. E-mail: axno@mcb.harvard.edu.

© 2005 by The National Academy of Sciences of the USA

supplemented with 10% FBS, antibiotics, and 5 units/ml IFN- γ . After 10 passages, IFN- γ was omitted from the medium.

Cell Culture. Medium A refers to DMEM (1 g of glucose per liter), plus antibiotics (100 units per ml of penicillin and 100 μ g per ml of streptomycin sulfate) and 10% FBS. Medium B refers to DMEM (4.5 g of glucose per liter) plus antibiotics and 10% FBS. Medium C is a 1:1 mixture of Ham's F12 medium and DMEM plus antibiotics. Medium D corresponds to medium C plus 10% FBS. 293 cells were maintained at 37°C in an atmosphere of 8% CO₂ in medium B. HD1A cells were maintained at 33°C in 8% CO₂ in medium D.

Phagocytosis Assays. Unless otherwise indicated, assays were performed with cells grown in poly(D-lysine)-coated 96-well plates (Becton Dickinson) using 0.773 \pm 0.014 μ m amine-coated latex beads (Polysciences). Beads were added from 25 μ g/ μ l stock suspensions (4 \times 10⁶ beads per μ g), and plates were centrifuged at 4°C for 5 min at 1,000 \times g and then incubated at 37°C as specified.

Lipid and Protein Analysis. Cells were washed with TBS and lysed in 0.5% (vol/vol) Nonidet P-40 plus protease inhibitors. Lysates from four wells were pooled and cholesterol was determined by using an Amplex Red Cholesterol Assay kit (Molecular Probes). Phospholipids were extracted with hexane/isopropanol (3:2) and quantified as described (9). Proteins were quantified by using a bicinchoninic acid kit (Pierce).

Quantitative Real-Time PCR. For each reaction cells from 10 wells of a 96-well plate were pooled and RNA was isolated by using Tri-reagent (Molecular Research Center). Two micrograms of total RNA were reverse transcribed by using an Omniscript RT kit (Qiagen). Real-time quantitative PCRs (20 μ l) were set up with 100 ng of cDNA, 0.25 μ M of each primer (Table 1, which is published as supporting information on the PNAS web site) and QuantiTect SYBR Green PCR kit reagents (Qiagen).

Immunofluorescence Microscopy. Cells were fixed with 4% (wt/vol) paraformaldehyde, permeabilized with 0.1% Triton X-100, and sequentially stained with anti-SREBP2 (IgG-1D2; 4 μ g/ml) and Alexa Fluor 488-conjugated donkey anti-mouse IgG (Molecular Probes; 1:400). Microscopy was performed on a Nikon Eclipse TE300 fluorescence microscope equipped with a \times 100 objective and a model 2.1.1 Spot RT monochrome camera.

Plasmids and Adenoviruses. pFAS-Luc (containing nucleotides -444 to +67 of the rat fatty acid synthase promoter) (kindly provided by H. S. Sul and M. Griffin, University of California, Berkeley) (10); pCMV-Insig1-Myc (kindly provided by R. A. DeBose-Boyd, University of Texas Southwestern Medical Center) (11); pCMV-P450-TM/BP2(555-1141) (12); pCMV-P450-TM/SCAP(731-1276) (12) and pSRE-Luc (13) have been described in the indicated references. phRL-CMV was from Promega. To generate pHMGCs-Luc a PCR fragment containing nucleotides -379 to -17 (Table 1) of the hamster 3-hydroxy-3-methylglutaryl (HMG) CoA synthase gene was cloned into the SmaI site of pGL2-basic (Promega). To generate pLDLR-Luc, a PCR fragment containing nucleotides -335 to +3 of the human LDL receptor gene (Table 1) was cloned into the SmaI site of pGL2-basic. pLDLR-Luc/*mut*SRE differs from pLDLR-Luc in one nucleotide in the SRE-1 sequence of the LDL receptor promoter (ATCACCCAC changed to ATAACCCAC) (14). To generate pENTR-IRES-EGFP, the BamHI-NotI fragment of pENTR1A (Invitrogen) was replaced with a fragment containing an IRES (derived from pIRESneo2, Clontech) followed by the coding sequence for EGFP (derived from pEGFP-N3, Clontech). pENTR-dnSCAP-IRES-EGFP was gen-

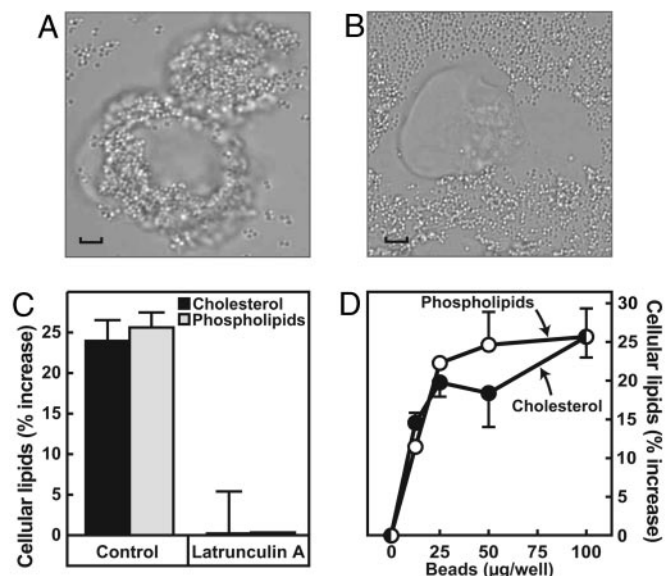


Fig. 1. Phagocytosis induces membrane lipid synthesis in human embryonic kidney 293 cells. On day 0, 293 cells were set up in medium A on coverslips in 24-well plates at 10⁵ cells per well (A and B) or in 96-well plates at 5 \times 10⁴ cells per well (C and D). (A and B) On day 2, cells were switched to medium D with 50 μ g per well of amine-coated latex beads, incubated for 6 h in the absence (A) or presence (B) of 1 μ M latrunculin A, washed, fixed, and analyzed by microscopy. (Bar, 2 μ m.) (C) On day 2, cells were incubated for 4 h in medium D plus or minus beads (100 μ g per well). Where indicated, 1 μ M latrunculin A was added 0.5 h before phagocytosis. Lipids were determined as described in *Materials and Methods* and corrected for protein concentration. Data indicate the concentrations of cholesterol and phospholipids expressed as % increase with respect to controls. (D) On day 2, cells were incubated for 4 h in medium D plus the indicated concentration of beads. Data are plotted as above. Lipid concentrations in control samples were 69.2 \pm 2.7 nmol cholesterol per mg protein and 218.6 \pm 3.6 nmol phospholipids per mg protein. Error bars indicate range ($n = 2$).

erated by cloning the BamHI-EcoRI fragment of pCMV-P450-TM/SCAP(731-1276) into the SmaI site of pENTR-IRES-EGFP. pENTR-Insig1-IRES-EGFP was generated by cloning the BamHI-EcoRI fragment of pCMV-Insig1-Myc into the SmaI site of pENTR-IRES-EGFP. pENTR-EGFP was generated by replacing the BamHI-NotI fragment of pENTR1A with the NheI-BglII fragment of pEGFP-C1 (Clontech). The adenoviral plasmids pAd-dnSCAP-IRES-EGFP, pAd-Insig1-IRES-EGFP and pAd-EGFP were generated by clone-mediated recombination using pAd/CMV/V5-DEST (Invitrogen) as acceptor and the pENTR1A-derived plasmids as donors.

Cell supernatants containing recombinant adenovirus were produced by using the Virapower Adenovirus Expression System (Invitrogen).

Reporter Gene Assays. Cells were transfected with 3 μ l of FuGENE 6 reagent (Roche Diagnostics) per μ g of DNA. Cells were lysed with 60 μ l per well of buffer A. Aliquots (20 μ l) were analyzed by using the Dual-Glo Luciferase Assay System (Promega).

For statistical analyses, sample sets were compared by paired, two-tailed Student's *t* test.

Results

Phagocytosis-induced membrane biogenesis was studied with human embryonic kidney 293 cells (15). Growth in the presence of 0.77- μ m amine-coated latex beads led to extensive accumulation of phagosomes in the cytoplasm (Fig. 1A). The intracellular localization of the beads was confirmed by staining with the

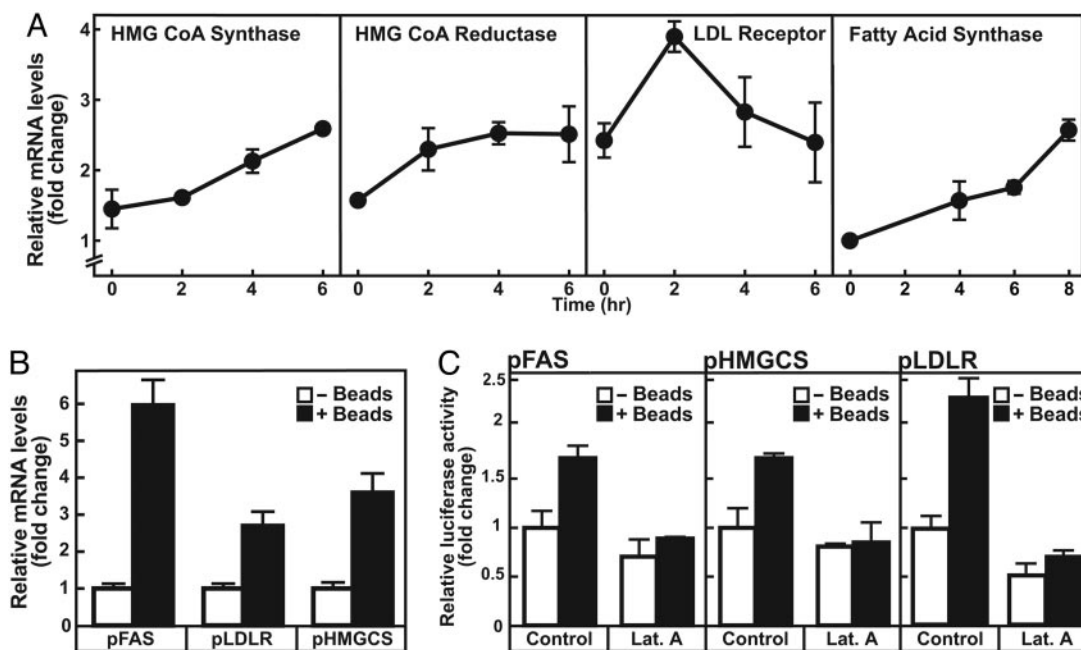


Fig. 2. Phagocytosis induces transcription of key genes required for lipid synthesis and uptake. On day 0, 293 cells were set up in medium A at 5×10^4 cells per well. (A) On day 2, cells were switched to medium D, incubated for 0.5 h plus or minus latex beads ($100 \mu\text{g}$ per well), washed, and incubated for the indicated time. Messenger RNAs were analyzed by quantitative real-time PCR. Data were normalized to the mRNA levels of TATA box binding protein and are expressed as fold change with respect to controls. (B) On day 1, 293 cells were transfected in medium A with 30 ng per well of pFAS-Luc (pFAS), pLDLR-Luc (pLDLR) or pHMGCS-Luc (pHMGCS). On day 2, cells were switched to medium D and incubated for 0.5 h plus or minus beads ($100 \mu\text{g}$ per well), washed, chased for 8 h in medium D, and then analyzed for luciferase activities. Data indicate firefly luciferase corrected for sea pansy luciferase and are expressed as fold change with respect to samples incubated without beads. (C) On day 1, 293 cells were transfected with pRL-CMV plus pFAS-Luc, pHMGCS-Luc, or pLDLR-Luc. On day 2, cells were incubated in medium D for 0.5 h plus or minus latex beads ($100 \mu\text{g}$ per well). Where indicated, wells received $1 \mu\text{M}$ latrunculin A (Lat. A) 0.5 h before phagocytosis. Cells were washed and chased in the absence of latrunculin A for 6 h in medium D. The three panels represent separate experiments. Luciferase activities are plotted as above. Error bars indicate SD ($n = 3$).

fluorescent lipid dye filipin, which indicated that each cell-associated bead was surrounded by a membrane (not shown). Moreover, no colocalization of cells and beads was seen in samples that had been incubated with latrunculin A (Fig. 1B), a drug that blocks phagocytosis by interfering with actin polymerization (16).

Because each phagosome is formed at the expense of $1.9 \mu\text{m}^2$ of membrane, we asked whether phagocytosis is followed by lipid synthesis. In confluent cultures of 293 cells that had been incubated with beads for 4 h, cholesterol and phospholipids increased by $\approx 25\%$ (Fig. 1C and D). Lipid concentrations remained unchanged when beads were added together with latrunculin A (Fig. 1C). In response to $100 \mu\text{g}$ of beads, cells synthesized 1.2 ± 0.03 nmol per well of phospholipids ($P < 0.02$) and 0.38 ± 0.01 nmol per well of cholesterol ($P < 0.01$) (Fig. 1D). Assuming a surface area of 0.55 nm^2 per phospholipid and 0.38 nm^2 per cholesterol molecule (17), the newly synthesized lipids can form a membrane bilayer of 242 nm^2 per well. This area is equivalent to the surface of 1.29×10^8 beads, or $30 \mu\text{g}$, which is close to the concentration of beads at which cells become saturated (Fig. 1D). From these data, we conclude that the cells synthesize lipids at amounts equal to those expended during phagocytosis.

Cholesterol can be produced by *de novo* biosynthesis or through hydrolysis of cholesteryl ester. Most carbon atoms in phospholipids are derived from fatty acids, which can also be generated through biosynthesis from acetyl CoA or by hydrolysis of triglycerides and cholesteryl ester. An important source of cholesteryl ester and triglycerides is low-density lipoprotein (LDL), which enters cells via the LDL receptor by clathrin-mediated endocytosis (18). Based on these considerations, we tested whether phagocytosis-induced membrane biogenesis in-

volves enhanced expression of the LDL receptor and of enzymes required for *de novo* synthesis of cholesterol and fatty acids.

Cells were exposed to beads for 30 min and chased for different periods of time, and several mRNA species were analyzed by real-time quantitative PCR. TATA box binding protein remained relatively unchanged under all conditions (not shown) and was thus chosen as a control for normalization. Significant increases were seen for the LDL receptor, two enzymes involved in cholesterol biosynthesis (HMG CoA synthase and HMG CoA reductase) as well as fatty acid synthase (FAS) (Fig. 2A). The LDL receptor responded most sensitively to phagocytosis, with mRNA levels being increased 2.4-fold only 30 min after addition of beads ($P < 0.008$). The LDL receptor mRNA reproducibly peaked at 2 h and then declined, whereas the mRNAs for HMG CoA synthase and FAS continued to increase.

Regulation is at least partly exerted on the level of transcription, as reporter gene constructs with the promoters for FAS, LDL receptor and HMG CoA synthase were also induced in response to beads (Fig. 2B). In the presence of latrunculin A bead-induced transcription was blocked, confirming a requirement for particle engulfment (Fig. 2C). In summary, the results in Fig. 2 demonstrate that membrane synthesis in response to phagocytosis correlates with increased transcription of genes required for the uptake and synthesis of cholesterol and fatty acids.

The parallel induction of several lipogenic proteins in response to beads suggested that phagocytosis might trigger the activation of a centrally acting transcription factor. One set of candidates is SREBPs. Members of the family are able to bind the promoters for all of the genes analyzed in Fig. 2 as well as to the promoters of several other genes required for the synthesis

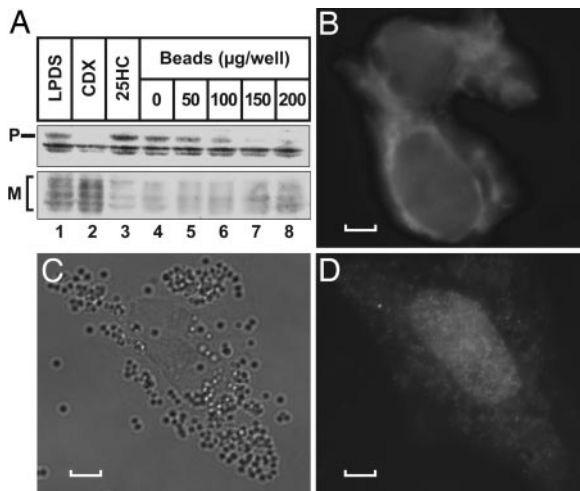


Fig. 3. Phagocytosis induces cleavage of SREBPs. (A) On day 0, 293 cells were set up in medium A at 5×10^4 cells per well. On day 2, cells were incubated for 4 h in medium C supplemented with 25 $\mu\text{g}/\text{ml}$ ALLN (Calbiochem) and the following: 10% LPDS and 5 μM compactin (lane 1); 10% LPDS, 5 μM compactin, and 1% (wt/vol) hydroxypropyl β -cyclodextrin (lane 2); 10% LPDS, 5 μM compactin, and 1 $\mu\text{g}/\text{ml}$ 25HC (lane 3); or 10% FBS plus the indicated concentration of beads (lanes 4–8). Total cell extracts (100 μg of protein per lane) were subjected to SDS/8% PAGE, transferred to nitrocellulose, and blotted with anti-SREBP-1 (IgG-2A4) as described (25). P and M denote the precursor and mature nuclear forms of SREBP-1, respectively. (B–D) On day 0, 293 cells were set up on coverslips in 24-well plates in medium A at 1×10^5 cells per well. On day 1, cells were incubated in medium D for 0.5 h plus (C and D) or minus (B) 50 μg per well of beads. Cells were then washed and incubated in medium D for 6 h. ALLN (25 $\mu\text{g}/\text{ml}$) was added during the last 4 h. Cells were stained with anti-SREBP-1 and fluorescently labeled anti-mouse IgG. (B and D) Fluorescence micrographs. (C) Bright field image. C and D show the same cell. (Bars, 2 μm .)

of cholesterol and fatty acids (19). Three SREBP isoforms have been identified: SREBP-1a, SREBP-1c/ADD1 and SREBP-2 (20–22). 293 cells express very little SREBP-1c/ADD1 and approximately equal amounts of SREBP-1a and SREBP-2 (23, 24). In the inactive state, SREBPs remain sequestered in the endoplasmic reticulum (ER) by virtue of two transmembrane domains. Upon activation, SREBPs are transported to the Golgi and cleaved by two sequentially acting proteases (11, 25, 26). Proteolysis releases the transcriptionally active N termini of SREBPs, which migrate to the nucleus.

To test whether phagocytosis-induced transcription involves the proteolytic activation of SREBPs, cells were grown in the presence of FBS and different amounts of beads for 4 h. Lysates were then analyzed by immunoblotting with an antibody directed against the N terminus of SREBP-1 (Fig. 3A). After growth in FBS alone, SREBP-1a remained largely in its membrane-bound precursor form (Fig. 3A Upper, lane 4) and only small amounts of the nuclear fragment were detectable (Fig. 3A Lower). Addition of beads led to a dose-dependent conversion of the SREBP-1a precursor to its smaller mature form (lanes 5–8). Similar results were obtained with an antibody against SREBP-2 (data not shown).

To verify whether phagocytosis-induced proteolysis leads to the transfer of SREBPs to the nucleus, cells were analyzed by immunofluorescence microscopy with an antibody against the N terminus of SREBP-2. In the absence of beads, SREBP-2 staining was predominantly extranuclear (Fig. 3B), reflecting its sequestration in the ER (21). After phagocytosis of latex beads, SREBP-2 was seen almost exclusively in the nucleus (Fig. 3D). Similar results were obtained with an antibody against SREBP-1

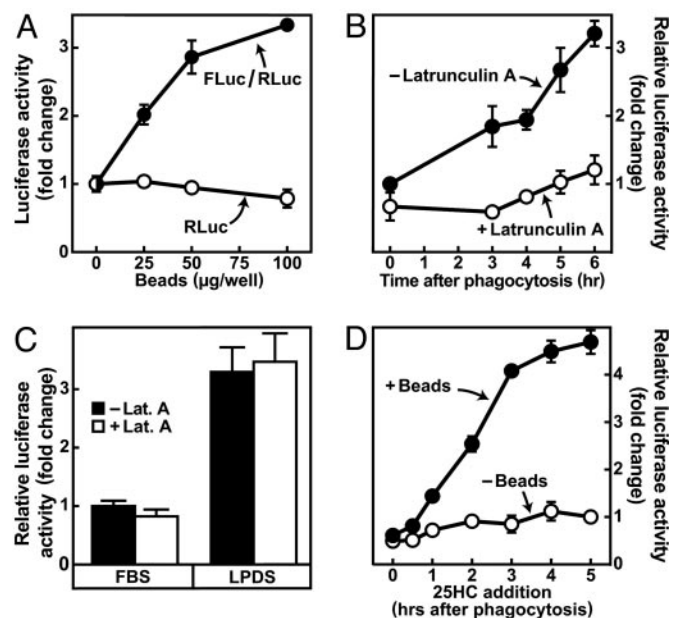


Fig. 4. Phagocytosis-induced activation of an SREBP-specific reporter gene. On day 0, 293 cells were set up in medium A at 5×10^4 cells per well. On day 1, cells were transfected with 30 ng per well of pSRE-Luc plus 30 ng of pSRE-Luc for 16 h. (A) After transfection, cells were switched to medium D and incubated for 0.5 h with the indicated concentrations of latex beads. Cells were washed, chased in medium D for 5 h, lysed, and analyzed for luciferase activities. Data indicate sea pansy luciferase (RLuc) or firefly luciferase corrected for sea pansy luciferase (FLuc/RLuc) and are expressed as fold change. (B) After transfection, 293 cells were switched to medium D/0.4% (vol/vol) DMSO with or without 1 μM latrunculin A for 0.5 h. Cells then received 100 μg per well of latex beads without change of medium. After 0.5 h, cells were washed and chased in medium D for the indicated time. Data are plotted as in Fig. 2B. (C) After transfection, cells were incubated for 6 h in medium C supplemented with 10% FBS or LPDS plus or minus 1 μM latrunculin A. Cells were then lysed and analyzed for luciferase activities. (D) After transfection cells were incubated in the absence or presence of latex beads (100 μg per well) for 0.5 h. Cells were washed (time 0), switched to medium D for 5 h, and analyzed for luciferase activities. During the 5-h period, 1 $\mu\text{g}/\text{ml}$ 25HC was added at the indicated time. Error bars indicate SD ($n = 3$).

(data not shown). Taken together these data demonstrate that phagocytosis triggers the proteolytic activation of SREBPs.

To address whether SREBPs released in response to phagocytosis are transcriptionally active, cells were transfected with an SREBP-specific reporter plasmid. This construct, pSRE-Luc, expresses firefly luciferase from three copies of a sterol regulatory element (13). After transfection, cells were exposed to different amounts of beads for 30 min, washed, and chased for 5 h. As shown in Fig. 4A, exposure of cells to beads led to a dose-dependent increase in luciferase activity. Increased expression of SRE-luciferase was also observed when silicate was used instead of latex beads, indicating that phagocytosis-induced transcription is independent of the particle composition (data not shown). Activation of transcription required bead internalization as luciferase activities remained low when phagocytosis was blocked by latrunculin A (Fig. 4B).

To rule out that latrunculin A might interfere with transcription in a phagocytosis-unrelated manner, we exploited the fact that SREBPs are also activated by cholesterol starvation (21). SREBP activity induced by growth of cells in cholesterol-poor medium for 6 h was indeed unaffected by the presence of latrunculin A (Fig. 4C).

The results in Fig. 4B indicated that SREBP activity was increased as early as 3 h after bead uptake. To analyze the kinetics of activation in greater detail, we took advantage of the

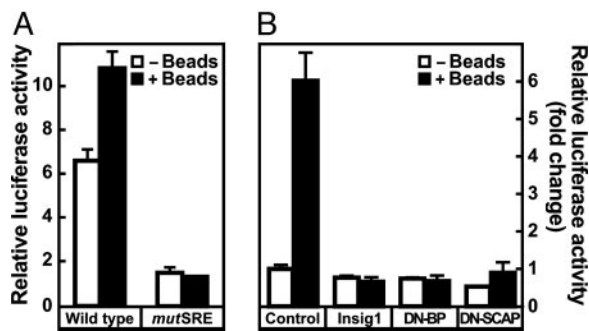


Fig. 5. SREBPs are required for phagocytosis-induced transcription. 293 cells were set up on day 0 in medium A at 5×10^4 cells per well. (A) On day 1, cells were transfected with 30 ng per well of pRL-CMV plus 30 ng per well of pLDR-Luc (*WT*) or pLDR-Luc/*mutSRE*. After 16 h, cells were incubated for 0.5 h in medium D plus or minus latex beads (100 μ g per well). Cells were washed and chased for 8 h. Data indicate firefly luciferase corrected for sea pansy luciferase and are expressed as fold change. (B) On day 1, cells were transfected with 20 ng per well of pRL-CMV plus 20 ng per well of pFAS-Luc. In addition, wells received 20 ng of either pCDNA3 empty vector (Control), pCMV-Insig1 (*Insig1*), pCMV-P450-TM/BP2(555–1141) expressing dominant negative SREBP-2 (DN-BP), or pCMV-P450-TM/SCAP (731–1276) expressing dominant negative SCAP (DN-SCAP). After 16 h, cells were incubated with beads, chased and analyzed as above. Error bars indicate SD ($n = 3$).

fact that proteolysis of SREBPs is efficiently blocked by 25HC (21, 25). Cells were transfected with pSRE-Luc and exposed to beads for 30 min. Subsequently, unincorporated beads were washed off, and all cells were chased for 5 h. When 25HC was added at 0 h of chase, luciferase activity remained at background levels (Fig. 4D). In comparison, luciferase levels increased by 40% when 25HC was added at 1 h of chase ($P < 0.006$). These results indicate that SREBPs are activated within 0–60 min of particle uptake. In summary, the results in Figs. 3 and 4 demonstrate that phagocytosis stimulates both the structural and functional activation of SREBPs.

We next asked whether SREBPs are required for phagocytosis-induced transcription of lipogenic enzymes. First, we studied a luciferase reporter gene that was driven from an LDL receptor promoter in which the SREBP binding site had been inactivated by a single point mutation (14). Compared to the wild-type construct, the mutant gene exhibited reduced basal expression and no increase in response to phagocytosis (Fig. 5A). Similar results were obtained with a construct in which the SREBP binding site had been mutated in the FAS promoter (27) (data not shown).

ER export and cleavage of SREBPs can be blocked by overexpression of one of three proteins: (i) the C-terminal cytosolic domain of SREBP-2, (ii) the C-terminal cytosolic domain of the SREBP escort protein SCAP, and (iii) *Insig1*, a protein required for retention of SREBP in the ER (11, 12). Cells were transfected with a luciferase reporter plasmid containing the promoter for FAS plus vectors expressing the inhibitory proteins listed above. In response to phagocytosis, luciferase levels in control samples were induced 6-fold (Fig. 5B). However, upon coexpression of *Insig1*, C-terminal SCAP or C-terminal SREBP-2, luciferase levels remained unchanged. Similar results were obtained when luciferase was expressed from an LDL receptor, HMG CoA synthase, or 3xSRE promoter (not shown). Taken together, these results support the conclusion that SREBPs are required for phagocytosis-induced transcription.

If SREBP-mediated transcription were required for membrane biogenesis, inhibition of the SREBP pathway should block phagocytosis-induced lipid synthesis. To test this prediction, we generated three recombinant adenoviruses expressing EGFP,

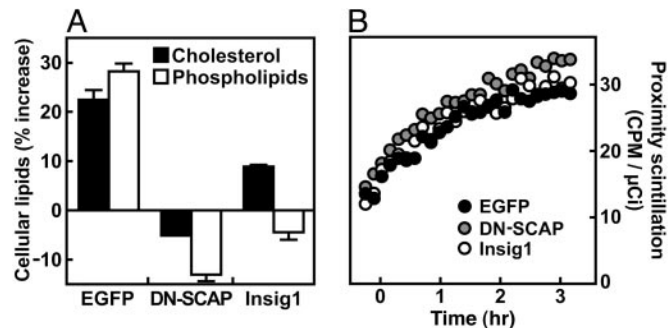


Fig. 6. SREBPs are required for phagocytosis-induced lipid synthesis. (A) On day 0, HD1A immortalized mouse macrophages were set up in medium D at 2×10^4 cells per well. On day 1, cells were infected with adenovirus encoding EGFP, dominant negative SCAP (DN-SCAP) or *Insig1* (*Insig1*) at a MOI of 250. On day 3, cells were incubated plus or minus 100 μ g per well of latex beads for 8 h. Cells were then harvested to determine lipid and protein concentrations. Data indicate the concentrations of cholesterol (black bars) and phospholipids (white bars) expressed as percent increase with respect to samples incubated without beads. Lipid concentrations in control samples were 237.7 ± 5.7 nmol of cholesterol per mg of protein and 758.2 ± 4.1 nmol of phospholipids per mg of protein. Error bars indicate SD ($n = 2$). (B) On day 0, HD1A cells were set up at 3×10^5 cells per well in a 24-well plate. On day 1, cells were infected with adenovirus expressing EGFP, dominant negative SCAP, or *Insig1* at a MOI of 250. On day 2, cells received liposomes containing [3 H]cholesteryl oleate (1 μ Ci per 0.5 ml per well; 1 Ci = 37 GBq). On day 3, cells were washed and incubated in fresh medium for 1 h. The dish was then placed on ice, and each well received 50 μ g of scintillant yttrium silicate beads for 30 min. Subsequently, the dish was transferred to a scintillation counter at 33°C and scintillation was measured every minute over a period of 3.5 h (28). Data represent the average of triplicate wells. Coefficients of variation ranged from 0.7 to 19.4%, with an average of 9.6%.

Insig1, and the C-terminal domain of SCAP. The viruses were then added to a line of immortalized mouse macrophages, HD1A cells that can be infected with close to 100% efficiency. After 2 days of infection, the cells were incubated in the absence or presence of beads for 8 h. In EGFP-transduced cells exposed to beads, phospholipids increased by 28% ($P < 0.007$) and cholesterol increased by 22% ($P < 0.02$) with respect to controls (Fig. 6A). By contrast, in cells expressing the C terminus of SCAP, phagocytosis led to a slight decrease of both cholesterol and phospholipid levels. After overexpression of *Insig1* phagocytosis-induced, cholesterol synthesis was significantly blunted and phospholipid levels decreased. To test whether expression of *Insig1* and C-terminal SCAP were interfering with particle uptake, the kinetics of phagocytosis were analyzed with a live-cell scintillation proximity assay. In this assay, photons are emitted as scintillant microspheres are enveloped with [3 H]cholesteryl-loaded plasma membrane (28). No significant differences were seen between samples expressing the three viruses (Fig. 6B). These data demonstrate that SREBPs are required for phagocytosis-induced membrane biogenesis.

Discussion

Here we show that phagocytosis triggers the proteolytic activation of SREBP transcription factors, their transport to the nucleus, enhanced transcription of lipogenic proteins, and the synthesis of cholesterol and phospholipids. Interference with SREBP activation blocked phagocytosis-induced transcription and lipid synthesis, indicating that SREBPs play an essential role in membrane biogenesis.

An important insight gained by these studies lies in the demonstration that SREBP-1a and SREBP-2 can be activated by general membrane demand rather than through lipid starvation. In 293 and other cultured mammalian cells, proteolysis of SREBP-1a and SREBP-2 has been shown to be induced by

cholesterol withdrawal (21, 29, 30). Moreover, growth in medium lacking unsaturated fatty acids promotes the activation of SREBP-1a and SREBP-1c/ADD1 (24, 31, 32).

The current experiments were performed in the presence of 10% serum, which provides and abundant source of cholesterol and fatty acids and usually suppresses the activation of all three SREBPs (ref. 24 and Fig. 3). Despite the presence of lipid-rich medium, phagocytosis led to proteolysis of SREBPs, transfer of the N-terminal fragments to the nucleus, and activation of an SREBP-specific reporter gene (Figs. 4 and 5).

The sequence of events leading from particle uptake to proteolysis of SREBPs is still incompletely understood. SREBP activation might involve phagocytosis-induced metabolism of unsaturated fatty acids or subcellular redistribution of cholesterol. In support of the latter possibility, we found that phagocytosis-induced SREBP activity was blocked under the same conditions that prevent SREBP activation in response to cholesterol deprivation, including (i) exposure of cells to 25HC, (ii) overexpression of Insig-1, (iii) overexpression of a dominant negative form of SREBP-2, and (iv) overexpression of a dominant negative form of SCAP (Figs. 4 and 5) (11, 12, 21). Although these results suggest that the phagocytosis and cholesterol-controlled pathways are largely overlapping, more studies will be required to elucidate the phagocytosis-induced initiation of SREBP cleavage.

Subsequent to phagocytosis-induced proteolysis, SREBPs direct the transcription of genes involved in the uptake and synthesis of membrane precursors. Inhibition of the SREBP pathway simultaneously blocked transcription and the synthesis of cholesterol and phospholipids (Figs. 5 and 6). Membrane biogenesis in response to phagocytosis appears to be under

feedback control as the amount of lipids synthesized closely matches the quantity of membranes that are used for particle engulfment (Fig. 1). Membrane biogenesis follows bead internalization with a lag period of at least 1 h, indicating that lipid synthesis is not required for the initial uptake phase (ref. 4 and data not shown). In macrophages, the principal source of membranes for phagocytosis of submicrometer latex beads are endosomes (3). For unknown reasons, the conversion from vesicles to phagosomes renders these membranes "invisible" to the homeostatic system, although all endosomal material remains inside the cell. Several studies have shown that phagosomes containing inert material rapidly lose the ability to fuse with other vesicles (33–35). It is possible that the practical removal of phagosomal membranes from vesicular trafficking pathways triggers membrane biogenesis until a functional system is restored. How such processes might relate to the regulation of lipid synthesis remains to be explored.

The activation of different lipogenic enzymes by one set of transcription factors provides a partial explanation for the problem of how the synthesis of many different lipids is coordinated during membrane biogenesis. However, fine-tuning of the membrane composition likely involves additional mechanisms for feedback and cross-regulation. Phagocytosis-induced membrane biogenesis should prove a useful system to further explore these problems.

We thank H. S. Sul, M. Griffin, R. A. DeBose-Boyd, Y. K. Ho, B. M. Spiegelman (Harvard Medical School, Boston), and J. Lin (Harvard Medical School) for kindly sharing reagents and Ashley Johnson for technical assistance. This work was supported by National Institutes of Health Grant R01 DK59934 and the Searle Scholars Program.

- Voelker, D. R. (2002) in *Biochemistry of Lipids, Lipoproteins and Membranes*, eds. Vance, D. E. & Vance, J. E. (Elsevier, Amsterdam), 4th Ed., pp. 449–482.
- Tartakoff, A. M., Gordon, S. & Dalbey, R. E., eds. (1999) *Phagocytosis: The Host* (Elsevier, Amsterdam).
- Aderem, A. (2002) *Cell* **110**, 5–8.
- Werb, Z. & Cohn, Z. A. (1972) *J. Biol. Chem.* **247**, 2439–2446.
- Sato, R., Yang, J., Wang, X., Evans, M. J., Ho, Y. K., Goldstein, J. L. & Brown, M. S. (1994) *J. Biol. Chem.* **269**, 17267–17273.
- Janowski, B. A., Shan, B. & Russell, D. W. (2001) *J. Biol. Chem.* **276**, 45408–45416.
- Goldstein, J. L., Basu, S. K. & Brown, M. S. (1983) *Methods Enzymol.* **98**, 241–260.
- Jat, P. S., Noble, M. D., Ataliotis, P., Tanaka, Y., Yannoutsos, N., Larsen, L. & Kiousis, D. (1991) *Proc. Natl. Acad. Sci. USA* **88**, 5096–5100.
- Zhou, X. & Arthur, G. (1992) *J. Lipid Res.* **33**, 1233–1236.
- Moon, Y. S., Latasa, M. J., Kim, K. H., Wang, D. & Sul, H. S. (2000) *J. Biol. Chem.* **275**, 10121–10127.
- Yang, T., Espenshade, P. J., Wright, M. E., Yabe, D., Gong, Y., Aebersold, R., Goldstein, J. L. & Brown, M. S. (2002) *Cell* **110**, 489–500.
- Sakai, J., Nohturfft, A., Goldstein, J. L. & Brown, M. S. (1998) *J. Biol. Chem.* **273**, 5785–5793.
- Hua, X., Nohturfft, A., Goldstein, J. L. & Brown, M. S. (1996) *Cell* **87**, 415–426.
- Briggs, M. R., Yokoyama, C., Wang, X., Brown, M. S. & Goldstein, J. L. (1993) *J. Biol. Chem.* **268**, 14490–14496.
- Graham, F. L., Smiley, J., Russell, W. C. & Nairn, R. (1977) *J. Gen. Virol.* **36**, 59–74.
- de Oliveira, C. A. & Mantovani, B. (1988) *Life Sci.* **43**, 1825–1830.
- Levine, Y. K. & Wilkins, M. H. (1971) *Nat. New Biol.* **230**, 69–72.
- Horton, M. S. & Goldstein, J. L. (1986) *Science* **232**, 34–47.
- Horton, J. D. & Shimomura, I. (1999) *Curr. Opin. Lipidol.* **10**, 143–150.
- Tontonoz, P., Kim, J. B., Graves, R. A. & Spiegelman, B. M. (1993) *Mol. Cell. Biol.* **13**, 4753–4759.
- Wang, X., Sato, R., Brown, M. S., Hua, X. & Goldstein, J. L. (1994) *Cell* **77**, 53–62.
- Hua, X., Yokoyama, C., Wu, J., Briggs, M. R., Brown, M. S., Goldstein, J. L. & Wang, X. (1993) *Proc. Natl. Acad. Sci. USA* **90**, 11603–11607.
- Ou, J., Tu, H., Shan, B., Luk, A., DeBose-Boyd, R. A., Bashmakov, Y., Goldstein, J. L. & Brown, M. S. (2001) *Proc. Natl. Acad. Sci. USA* **98**, 6027–6032.
- Hannah, V. C., Ou, J., Luong, A., Goldstein, J. L. & Brown, M. S. (2000) *J. Biol. Chem.* **276**, 4365–4372.
- Nohturfft, A., Yabe, D., Goldstein, J. L., Brown, M. S. & Espenshade, P. J. (2000) *Cell* **102**, 315–323.
- Sakai, J., Duncan, E. A., Rawson, R. B., Hua, X., Brown, M. S. & Goldstein, J. L. (1996) *Cell* **85**, 1037–1046.
- Lin, J., Yang, R., Farr, P. T., Wu, P. H., Handschin, C., Li, S., Yang, W., Pei, L., Uldry, M., Tontonoz, P., et al. (2005) *Cell* **120**, 261–273.
- Stockinger, W., Castoreno, A. B., Wang, Y., Pagnon, J. C. & Nohturfft, A. (2004) *J. Lipid Res.* **45**, 2151–2158.
- Yang, J., Brown, M. S., Ho, Y. K. & Goldstein, J. L. (1995) *J. Biol. Chem.* **270**, 12152–12161.
- Hua, X., Sakai, J., Brown, M. S. & Goldstein, J. L. (1996) *J. Biol. Chem.* **271**, 10379–10384.
- Thewke, D. P., Panini, S. R. & Sinensky, M. (1998) *J. Biol. Chem.* **273**, 21402–21407.
- Worgall, T. S., Sturley, S. L., Seo, T., Osborne, T. F. & Deckelbaum, R. J. (1998) *J. Biol. Chem.* **273**, 25537–25540.
- Montgomery, R. R., Webster, P. & Mellman, I. (1991) *J. Immunol.* **147**, 3087–3095.
- Oh, Y. K. & Swanson, J. A. (1996) *J. Cell Biol.* **132**, 585–593.
- Desjardins, M., Nzala, N. N., Corsini, R. & Rondeau, C. (1997) *J. Cell Sci.* **110**, 2303–2314.